# Scaling relations in the Lyapunov exponents of one dimensional maps

P R KRISHNAN NAIR*, V M NANDAKUMARAN and G AMBIKA*
Department of Physics, Cochin University of Science and Technology, Cochin 682 022, India
*Permanent Address: Department of Physics, Maharajas College, Cochin 682 011, India

**Abstract.** We establish numerically the validity of Huberman–Rudnick scaling relation for Lyapunov exponents during the period doubling route to chaos in one dimensional maps. We extend our studies to the context of a combination map, where the scaling index is found to be different.

## 1. Introduction

The behaviour of nonlinear dynamical systems can be analysed most extensively using one-dimensional iterative maps. These maps undergo a transition from regular to chaotic behaviour at certain values of the system parameter; the most prominent route for this transition being the period doubling scenario [1]. Studies related to the universal nature of indices associated with this scenario have resulted in the classification of one-dimensional maps into different universality classes, based on $z$, the order of the maximum of the map [2]. The chaotic state is detected most often, using an index called the Lyapunov characteristic exponent ($\lambda$). It gives a quantitative measure of the average separation of two initially close orbits as the system evolves in time. A positive value for $\lambda$ is an unambiguous signature of chaos while a negative value implies periodic or quasiperiodic behaviour in the system. As such, $\lambda$ can be referred to as an order parameter in the transition from periodic to chaotic state. In this context, the scaling behaviour of $\lambda$ during the transition from order to chaos is important and interesting in understanding the onset of chaos in the system. The nature of this scaling near the period doubling accumulation point has been theoretically worked out for one dimensional maps by Huberman and Rudnick [3]. They have shown that the Lyapunov characteristic exponent follows the relation,

$$\lambda \propto |a - a_\infty|^\nu \tag{1}$$

where $a_\infty$ is the value of the control parameter $a$ at the period doubling accumulation point and

$$\nu = \frac{\ln 2}{\ln \delta} \tag{2}$$

421

$\delta$ being the Feigenbaum universality constant. This scaling law in the context of quadratic maps has been verified experimentally using a sinusoidally driven diode circuit [4]. A scaling theory for noisy period doubling transition to chaos has been developed by Shraiman *et al* [5] in which it is shown that in the limit of the noise amplitude tending to zero, the Huberman-Rudnick [H-R] relation is recovered.

The H-R relation indicates that the exponent $v$ depends on $z$ through $\delta$ which is different for different universality classes. However, it is not clear whether $v$ may depend on $z$ in some other way. To the best of our knowledge, no numerical investigations have been reported for $z$ other than 2. In this paper, we report the results of a detailed numerical study of the scaling law near $a_\infty$ in one dimensional maps for different $z$ values. We prove the universal validity of the H-R relation and at the same time extend the studies to combination maps. Such maps, when combined using maps belonging to the same universality class and therefore with the same $\delta$ value are found to have different scaling indices.

This paper is organized as follows. In §2 we give the details of our numerical analysis for maps of different universality classes. The period doubling accumulation point $a_\infty$ for different $z$-values are determined and the nature of the scaling of $\lambda$ obtained by plotting $\log \lambda$ against $\log |a - a_\infty|$. In §3 we extend the analysis to a combination map defined there. The salient features of this map during the onset of chaos and the scaling of its $\lambda$ are included. Our concluding remarks and comments are given in §4.

## 2. Scaling law for general one-dimensional maps

We start by considering maps of the form,

$$X_{n+1} = 1 - a_1 |X_n|^z \tag{3}$$

defined on the interval $(-1, 1)$, with the control parameter $a_1$ lying between 0 and 2. This is a unimodal map with the critical point $X_c = 0$; $z$ denotes the order of the maximum at $X_c$. This map can be transformed into one on the unit interval $(0, 1)$ by a nonlinear transformation [1].

The transformed map then becomes

$$X_{n+1} = f(X_n) = \left(\frac{a}{4}\right) - 2^{(z-2)}a \left|X_n - \frac{1}{2}\right|^z \tag{4}$$

with $0 < a < 4$ and $X_c = \frac{1}{2}$.

The Lyapunov characteristic exponent in the context of such maps is defined as

$$\lambda = \lim_{N \to \infty} \frac{1}{N} \sum_{i=0}^{N-1} \ln |f'(X_i)| \tag{5}$$

This can be used as such in the computation of $\lambda$ for different $z$-values [6]. However, a numerical analysis poses the following difficulties. Since round off errors may possibly build up in a computer, $\lambda$ can be computed only by setting an upper bound for $N$ which may lead to some truncation error. In our computations $N$ is fixed as 10,000. Again the proximity of a large number of periodic windows within the chaotic regime near the accumulation point reduces the number of useful values of $\lambda$, especially for large values of $z$. But this can be overcome to some extent by adding a very weak
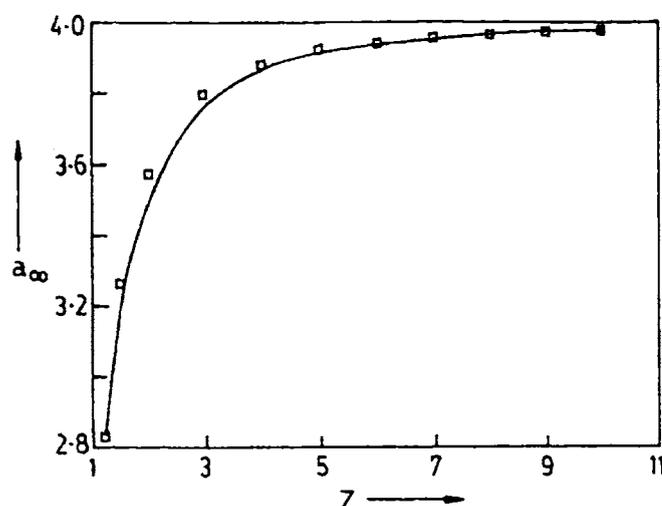
**Figure 1.** Variation of $a_\infty$ with $z$, the order of the maximum of the map. Note that as $z$ increases, the chaotic regime $a_\infty < a < 4$ shrinks and becomes very narrow for $z > 10$.

noise to the system. Such a noise term smoothens the curve for $\lambda$ against $a$ [7]. Thus for high values of $z$, we added a small amplitude noise term $\approx 10^{-15}$, for computational purposes.

Starting with $z = 1.2$, the $\lambda$ values for the map (4) are computed with values of $a$ increased in small steps. The value of $a_\infty$ at which transition to chaos is roughly estimated as that value of $a$ at which $\lambda$ changes from negative to positive value for the first time. Then the value of $a$ is varied in further small steps around this rough estimate and a better value for $a_\infty$ is obtained. Continuing this process, the value of $a_\infty$ is determined up to an accuracy of $10^{-6}$–$10^{-8}$. The Lyapunov characteristic exponent $(\lambda)$ is then computed for a number of values of $a > a_\infty$ and very near to $a_\infty$. This was repeated for different $z$-values.

For higher values of $z, \lambda$ in the chaotic side near $a_\infty$ changes to negative values quite often. This is due to the presence of a large number of periodic windows in the chaotic regime. The variation of $a_\infty$ with $z$ is sketched in figure 1. For large $z$, the value of $a_\infty$ approaches the fully chaotic limit $a = 4$ and the entire chaotic regime shrinks to a narrow region in the parameter space. Since the chaotic regime has to accommodate all the periodic windows, it is clear that a large number of periodic windows will be found near $a_\infty$, especially for high values of $z$. The addition of a small noise can wash out the fine structure of the periodic windows in the chaotic region. For $z \geqslant 2$, we added a Gaussian noise of zero mean and variance 0.2. The typical strength for the noise amplitude was $10^{-15}$. Such a low noise cannot seriously affect the scaling behaviour of the system. It is to be emphasized that even with noise, the problem of periodic windows cannot be completely overcome. Thus for very high $z$-values $(z \geqslant 4)$, we report the envelope scaling for $\lambda$, with the periodic windows avoided.

For each value of $z$, we obtain a plot of $\log \lambda$ against $\log|a - a_\infty|$ and the line of best fit is drawn. Its slope gives an estimate of $v$. A typical log–log plot is presented in figure 2. From the available values of $\delta$ for different $z$-values [8], the theoretical value for $v$ using (2) is calculated. These results are compared in table 1. Giving
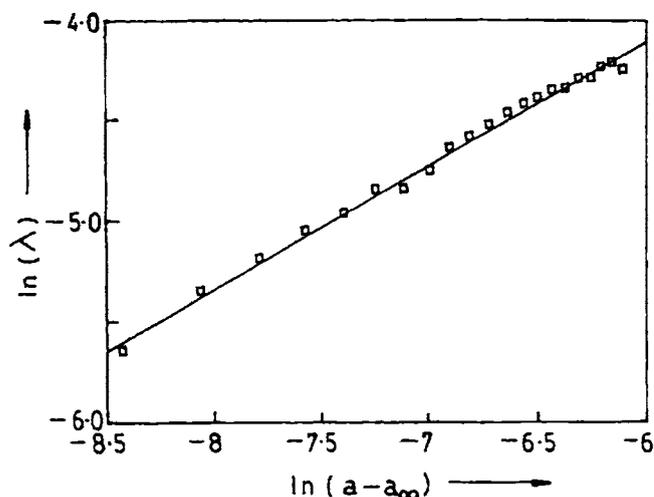
**Figure 2.** A typical log–log plot of $\lambda$ vs $(a - a_{\infty})$ for $z = 1\cdot2$. The slope of the line gives the scaling exponent $\nu$.

**Table 1.** The scaling index $\nu$ for different values of $z$, calculated numerically and using H–R relation.

| Order of maximum ($z$) | $\nu$ (numerical) | $\nu$ (using H–R) $= (\ln 2/\ln \delta)$ |
|---|---|---|
| 1·2 | 0·60171 | 0·6057799 |
| 1·5 | 0·52281 | 0·5192090 |
| 2·0 | 0·42117 | 0·4498200 |
| 3·0 | 0·40711 | 0·3834490 |
| 4·0 | 0·30117 | 0·3489280 |
| 5·0 | 0·29953 | 0·3266080 |

allowance for possible computational errors, we can say that there is excellent agreement with the H–R scaling relation.

### 3. Combination of two maps of the quadratic family

We consider the dynamics of a combination map obtained by combining a sinusoidal map with the well known logistic map. This map is thus an example of a two parameter one dimensional map and is given by,

$$X_{n+1} = f(X_n, \mu, A) = \mu X_n(1 - X_n) - A \sin(\pi X_n). \tag{6}$$

Here both the maps $f_1(X_n, \mu) = \mu X_n(1 - X_n)$ and $f_2(X_n, A) = A \sin(\pi X_n)$ belong to the same universality class viz, the quadratic family.

The map defined in (6) has an extremum at $X = \frac{1}{2}$ which is a second order maximum for $A$ ranging from $(\mu/4 - 1)$ to $(2\mu/\pi^2)$ while it is a minimum for $2\mu/\pi^2 < A < \mu/4$. Thus there is a point of inflexion at $X = 1/2$ when $A = 2\mu/\pi^2$. Consequently $f(X_n, \mu, A)$ is one humped for $(\mu/4 - 1) < A < 2\mu/\pi^2$ and two humped for $2\mu/\pi^2 < A < \mu/4$. For
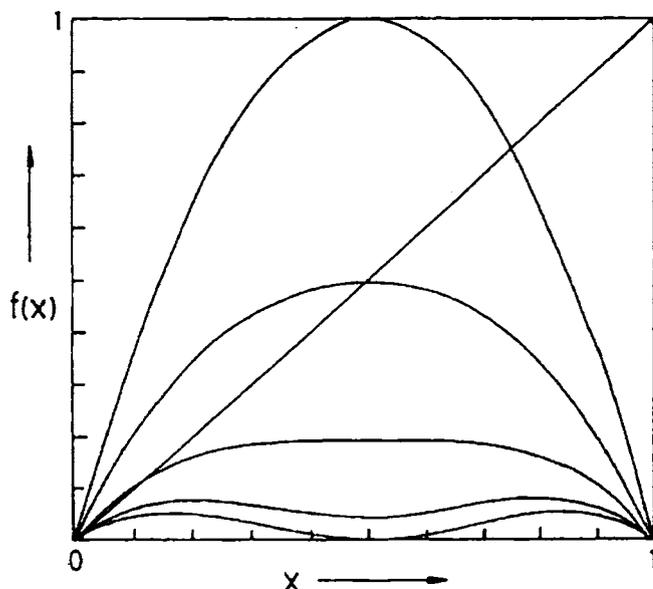
**Figure 3.** The combination map $f(X)$ given in (6) for $\mu = 4$. The curves correspond to $A = 0$, $0.5$, $8/\pi^2$, $3/\pi$ and 1 in that order from top to bottom.

any value of $\mu$, the corresponding minimum value for $A$ is $(\mu/4 - 1)$ and this occurs as $f(X_n, \mu, A)$ becomes equal to 1. Likewise the maximum value of $A$ for a given value of $\mu$ is $\mu/4$ which occurs as $f(X_n, \mu, A)$ becomes equal to zero. These features are made evident in figure 3 where $f(X_n, \mu, A)$ is plotted as a function of $X_n$ for different values of $A$, keeping $\mu = 4$. We thus observe that the parameter $A$ must lie between $(\mu/4 - 1)$ and $(\mu/4)$ so as to keep the iterates of the combined map within the unit interval $(0, 1)$.

With $\mu$ fixed at 4, we do a detailed numerical analysis of the system in (6). The parameter $A$ is increased slowly in steps of $0.001$ and a bifurcation diagram is drawn (figure 4). It is interesting to note that the system retraces the entire period doubling route to chaos in the reverse order as $A$ is slowly tuned and finally settles down to a one cycle for $A \geqslant 0.2435$. Here, the effect of the combination of the sinusoidal term to the logistic one is to reduce the height of the maximum at $X = 1/2$ as the parameter $A$ is increased, as is clear from figure 3. Further, if we start from a value of $\mu$ corresponding to one of the periodic cycles of the logistic map, by applying a negative value for $A$, the system can be brought to chaotic state.

It can be shown that in the one humped region of the map viz, $(\mu/4 - 1) < A < 2\mu/\pi^2$, the Schwarzian derivative of the function $f(X_n, \mu A)$ is negative over the entire range $(0, 1)$ for $X$. This means that period doubling is generic in the system [9].

By changing the value of $\mu$, a parameter space plot for the system is drawn (figure 5). This gives details regarding the transition from chaos to order and vice versa. For each chosen value of $\mu$, the Lyapunov characteristic exponent is calculated by varying $A$ in steps of $0.001$ and $A_\infty$ is determined as before. The thick line that represents the values of $A_\infty$ for each value of $\mu$ is thus the transition line between order and chaos. The lines parallel to it (only two are shown in figure 5) represent the bifurcation curves along which each period doubling occurs. The shaded region corresponds to the chaotic regime of the system, where the L.C.E is generally positive, except for windows of periodicity within the chaotic regime. The lowermost line corresponds
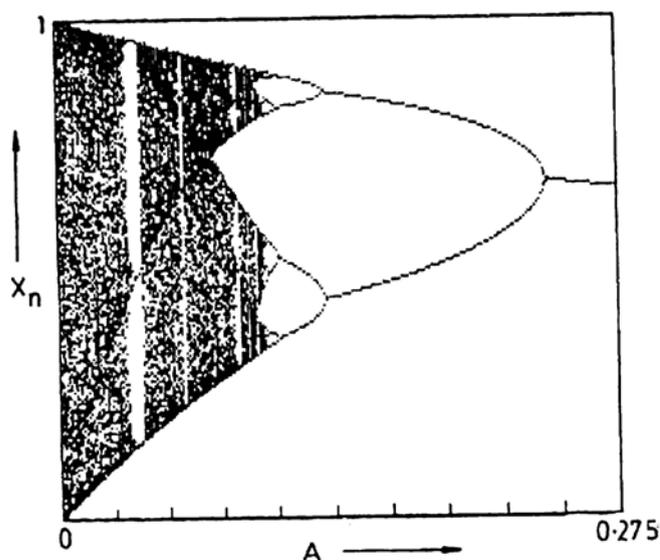
**Figure 4.** Bifurcation structure of the map in (6). With $\mu = 4$ and $A = 0$, the system is fully chaotic. As $A$ is slowly tuned, periodic cycles are traced in the reverse direction.
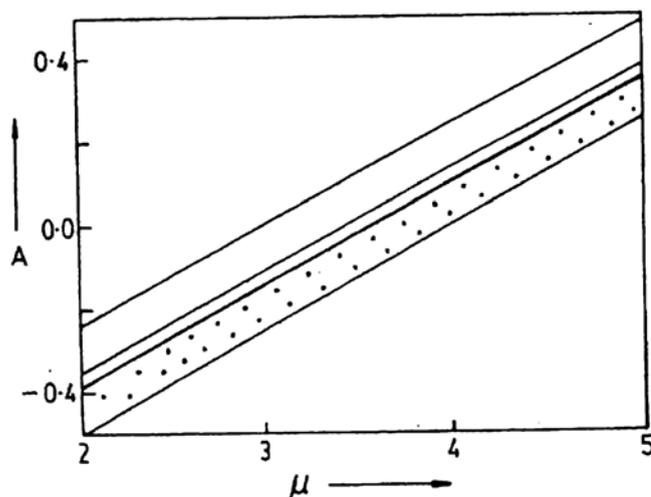


**Figure 5.** The parameter space $(\mu, A)$ of the combination map. The thick line represents the transition from order to chaos while the lines parallel to it, are the bifurcation curves.

to $A = (\mu/4 - 1)$. By extending this line upwards, we observe that we can increase the value of $\mu$ beyond $\mu = 4$ also, by taking suitable high values for $A$.

Since the bifurcation curves in the parameter space $(\mu, A)$ are parallel lines, it is clear that the Feigenbaum index $\delta$ defined in terms of the bifurcation values $A_n$ for fixed $\mu$, must be the same as the $\delta$ for the logistic map alone.

*Scaling of the Lyapunov exponent*

In order to investigate the scaling behaviour of $\lambda$ for the combination map, we use the same numerical procedure discussed in §2. Keeping the value of $\mu = 4$, $\lambda$ for the

**Table 2.** The scaling index $\nu$ and accumulation point $A_\infty$ for the combination map considered in §3, for various values of $\mu$.

| $\mu$ | $A_\infty$ | $\nu$ |
|------|------------|-------|
| 3·0 | − 0·1382968450 | 0·9989838 |
| 3·5 | − 0·0170178750 | 0·9677731 |
| 4·0 | 0·1046909450 | 0·9936844 |
| 32 | 7·2212675805 | 0·9996790 |

system is computed by slowly varying the parameter $A$. This enables us to obtain the value of $A_\infty$, the parameter value at which transition from chaos to order occurs, up to an accuracy of $10^{-8}$. Then the value of $A$ is varied in steps of $10^{-8}$ around $A_\infty$ and the corresponding values of $\lambda$ are determined. The slope of the line of best fit obtained by plotting $\log|\lambda|$ against $\log|A - A_\infty|$ is determined as the scaling index $\nu$. This is repeated for $\mu = 3\cdot5$ and 3 also. We then extend the investigations for a very high value of $\mu$ namely $\mu = 32$. Here, the parameter $A$ can vary from 7 to 8. In the latter case, the combination map is two humped from the very beginning. The results are presented in table 2.

From table 2, it is clear that in all the cases studied for the combination map, the scaling index is entirely different from that for the logistic map. The scaling index for the combination map is almost unity for all the cases considered. It is to be noted that this map has the same $\delta$ as the quadratic map. This would mean that the scaling relation in this case does not follow the H–R law. From the log–log plot for the combination map given in figure 6, it is evident that the points lie exactly along a straight line. The proximity of the periodic windows does not seem to hinder the numerical computations in this case. This could mean that periodic windows are less in number or they have been smeared out by the additional term in the map.

In an attempt to see why the combination map does not follow the H–R scaling relation, we carried out a detailed numerical analysis of the chaotic regime of the map. The control parameter $A$ is slowly and carefully varied and a series of bifurcation
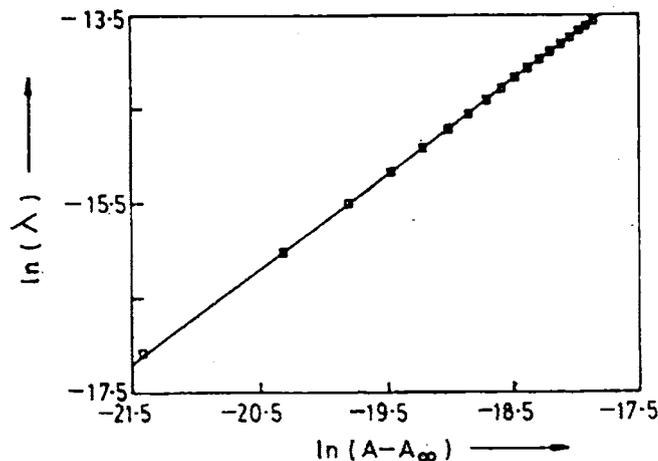


**Figure 6.** The LCE scaling for the combination map, $\ln|A - A_\infty|$ is plotted against $\ln|\lambda|$. Here, the value of $\mu = 32$. $\nu$ in this case is found to be $\approx 1$.

**Table 3.** Parameter values for successive bifurcations of the chaotic band of the combination map and its convergence rate $\delta_n$.

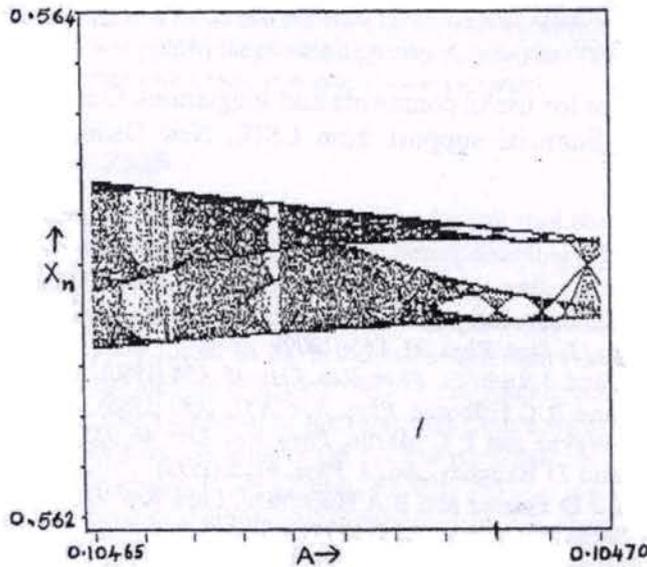| Parameter value $(A_n)$ | Convergence rate $\delta_n$ |
|---|---|
| 0·07909091 | — |
| 0·09954546 | — |
| 0·10360000 | 5·0449130 |
| 0·10444000 | 4·8267857 |
| 0·10463500 | 4·3076923 |
| 0·10467600 | 4·7560975 |
| 0·10468445 | 4·8235300 |
| 0·10468625 | 4·7222222 |



**Figure 7.** The band structure of the combination map on an enlarged scale. As $A$ increases towards $A_\infty$, merging of bands take place.

diagrams are drawn on an enlarged scale. This enabled us to observe the fine structure of the chaotic bands. With $\mu = 4$ and $A = 0$, the system is in the fully chaotic state. As $A$ is increased towards $A_\infty$, the chaotic band undergoes a series of bifurcations. After each bifurcation, one of the branches is taken and the bifurcation diagram is drawn on an enlarged scale. The control parameter is increased in very small steps and the next bifurcation point is obtained. Continuing this process, we could trace out the values of $A$ up to the 8th stage of band bifurcation. The values of $A$ at which successive band bifurcations occur and the convergence rate $\delta_n$ calculated in terms of these $A$-values are presented in table 3. With further increase of the control parameter $A$ towards $A_\infty$, recombination of bands is seen. Figure 7 shows the corresponding bifurcation diagram, in which merging of bands can be seen. Thus it is clear that in the case of the combination map, band bifurcation does not take place

ad infinitum. This incomplete nature of the cascade of bifurcations in the case of the combination map could be the possible reason for the scaling behaviour of its Lyapunov characteristic exponent ($\lambda$) to be different from the H–R law.

## 4. Concluding remarks

The work presented above establishes the validity of Huberman–Rudnick scaling law for different universality classes of one dimensional maps. However, we also find that it is possible to consider certain combinations of maps for which the Huberman–Rudnick law is not obeyed, as far as the scaling of the Lyapunov characteristic exponent is concerned. These combination maps have almost the same bifurcation structure as single maps. But our investigations indicate that the behaviour of the combination map in the immediate neighbourhood of $A_\infty$ is entirely different. What we observe is a series of band splittings and mergings before the system enters the periodic region. The exact reason as to why the cascade of band bifurcations is not complete is not yet clear. This is currently being investigated.

## Acknowledgements

## References

[1] G Ambika and K Babu Joseph, *Pramana – J. Phys.* 39, 193 (1992)
[2] M J Feigenbaum, *J. Stat. Phys.* 21, 665 (1979)
[3] B A Huberman and J Rudnick, *Phys. Rev. Lett.* 45, 154 (1980)
[4] S C Johnstone and R C Hilborne, *Phys. Rev.* A37, 2680 (1988)
[5] B Shraiman, E Wayne and P C Martin, *Phys. Rev. Lett.* 46, 935 (1981)
[6] J C Earnshaw and D Haughey, *Am. J. Phys.* 61, 5 (1993)
[7] J P Crutchfield, J D Farmer and B A Huberman, *Phys. Rep.* 92, 45 (1982)
[8] B Hu and I I Satija, *Phys. Lett.* A98, 143 (1983)
[9] H G Schuster, *Deterministic chaos*, (Physik Verlag, Weinheim, 1984)

154